High Sensitivity Biosensing Based on Symmetric Coupled Cavity Structure of Photonic Crystal Microcavities

Cheng-Chih Hsieh[1], Swapnajit Chakravarty[2], Yi Zou , Liang Zhu and Ray T. Chen[1]

[1]*Dept. Electrical and Computer Engineering, The University of Texas at Austin, 10100 Burnet Rd, PRC/MER 160, Austin, TX 78758, USA.*

[2]*Omega Optics, Inc., 10306 Sausalito Dr, Austin, TX 78759, USA.*

andreashsieh@utexas.edu, swapnajit.chakravarty@omegaoptics.com, raychen@uts.cc.utexas.edu, Fax: +1-512-471-8575

Abstract: We demonstrate that coupled cavity-waveguide architectures can lead to enhanced experimentally measured detection limit of 300 fM (20pg/ml) for sensing the binding of avidin to biotin in photonic crystal micro-cavity based biosensor.

OCIS Codes: (280.0280) Remote sensing and sensors (050.5298) Photonic crystals

Photonic crystal (PC) microcavities have attracted significant interest in label-free bio-sensing. To achieve label-free bio-molecule detection, several groups have investigated various platforms based on ring-resonators [1], wire waveguides [2], surface plasmon resonance (SPR) [3]. All the above methods are based on the specific binding of the biomolecule of interest to its conjugate biomolecule capture agent bound to the optical device. The photonic crystal microcavity structure we design is based on W1 line defect waveguide with lattice constant *a*, where W1 denotes the width of PCW is $\sqrt{3}a$. The air hole diameter is d=216 nm and silicon slab thickness is h=0.58a. PC L-type couple microcavities with length L21 are fabricated, where Ln denotes numbers of missing holes inside the cavity along Γ–K direction, and coupled cavities are designed two periods away from the W1 line defect at each side which is shown in Fig. 1.Coupled microcavities structure has two symmetric L21 microcavity at both sides of W1 waveguide, while previous designs [4] only include single cavity adjacent to W1 waveguide.

The total quality factor Q_T of the resonance mode of a PC microcavity, which is related to the photon lifetime τ_p, at frequency ω by $Q_T=\omega\tau_p$ is given by

$$\frac{1}{Q_T}=\frac{1}{Q_R}+\frac{1}{Q_i} \quad \ldots\ldots\ldots\ldots\ldots (1)$$

where $Q_R=\omega\tau_R$ and $Q_i=\omega\tau_i$, τ_R and τ_i represent the radiation loss and intrinsic cavity loss respectively. τ_R is given by:

$$\frac{1}{\tau_R}=\frac{P_R}{W_E} \quad \ldots\ldots\ldots\ldots\ldots\ldots (2)$$

where P_R denotes the total power radiated by the cavity and W_E denotes the stored energy in the cavity which is proportional to the cavity mode volume. Hence a method that reduces P_R and increases W_E will decrease the radiation loss from the cavity and hence increase the effective Q. A high Q implies that the light is trapped for a longer period of time in the cavity and hence interacts longer with any analyte in the vicinity of the photonic crystal microcavity. In addition, since W_E is proportional to the optical mode volume, a higher W_E leads to potential for larger optical mode overlap with the analyte which also contributes to higher sensitivity. In addition, increasing the length of the PC microcavities reduced the radiation loss, which scales inversely with the cavity length, thereby reducing the resonance linewidth and thus increasing the ability to detect small changes in concentration. Thus L21 type microcavities are presented in our work. Compared with single L21 cavity, L21 coupled cavities increase W_E by providing larger optical mode volume, and L21 couple cavities have better sensitivity since larger optical mode overlap gives stronger light-matter interaction with analyte. The increased length of the PC microcavities doesn't contradict the goal of chip-scale miniaturization, since a primary requirement this architectures is the need to functionalize the resonators with target receptor biomolecules that will bind specifically to their probe biomolecule conjugates in a diagnostic assay. The ink-jet printed target receptor spot size we achieved is about 35 mm in diameter [5], which thus determines the minimum spacing that can be achieved between adjacent resonators functionalized with different unique target receptor biomolecules.

We selected biotin as target receptor and avidin as probe protein. The dissociation constant (K_d) of the conjugate pair, avidin-biotin is about $10^{-15}M$. Wafers were functionalized by treating with 10% by volume 3-APTES in toluene. It is then washed 3 times in toluene to remove unbound 3-APTES, 3 times in methanol to remove toluene and finally 3 times in de-ionized water to remove methanol. The wafers are then incubated in 1% glutaraldehyde in phosphate buffered saline (PBS) for 5 min and washed 3 times in PBS and ink-jet printed with target antibodies in glycerol. The printed spots were left to incubate overnight. Subsequently, all target antibodies not bound to the

functionalized device layer were removed by washing 3 times in PBS. After overnight incubation and washing, the device is coated with bovine serum albumin (BSA) to prevent any non-specific binding and washed 3 times with PBS. The device is now ready for measurements.

Light is guided in and out of the PCW by ridge waveguides with PC group index taper to enable high coupling efficiency into the slow light guided [6]. The bottom cladding of silicon dioxide (n= 1.46) is kept intact to enable robust devices with high yield. Devices were tested with TE-polarized light by subwavelength grating coupling method [7] with polarization maintaining single mode tapered lensed fiber. All probe antibodies are introduced in PBS which forms the top cladding. When probe antibody that is specific to its conjugate target antibody is introduced, the conjugate specific binding causes a change in the refractive index in the immediate vicinity of the corresponding PC microcavity leading to a change in resonance frequency and hence a shift in wavelength of the dropped resonance from the transmission spectrum of the PCW. The resonance spectrum of the L21 PC couple microcavities were first measured in PBS, functionalized with target receptor. The transmission spectrum of the OCSS with the coupled L21 PC couple microcavities is shown in Fig. 2. The resonance wavelength is at 1558.9 nm, near the band edge at 1563 nm, with approximately 4 dB extinction ratio. the resonance wavelength range to show the Q~6000 in these devices in PBS, after functionalization with target receptor antibodies, in the absence of any probe antibodies. Before a new addition of antibody solution carrying probe protein, the resonance wavelength was measured (λ_1). For each concentration of newly added probe antibody solution, the chip was incubated in the probe antibody solution and the resonance wavelength monitored as a function of time. No resonance wavelength shift was observed for 20 min. After 20 min, the resonance wavelength increased as a function of time, until the shift saturated after another 20 min at λ_2. The chip was next washed 3 times in PBS to remove unbound probe Abs and the resonance wavelength $\lambda 3$ ($< \lambda 2$) measured again. The final resonance wavelength shift, $\Delta\lambda$, as plotted in Fig. 3 is given by $\Delta\lambda = \lambda_3 - \lambda_1$. Fig. 4 shows experimental resonant transmission spectra observed when avidin binds to the target biotin at low concentrations from 300fM to 1pM. The new symmetric dual L21 coupled cavity outperforms previous single L21 coupled cavity designs [8], which demonstrated detection limit at 1 pM.

In summary, we demonstrated here that high sensitivity photonic crystal microcavity biosensors in silicon-on-insulator substrates can be realized by engineering the radiation loss and the optical mode volume in addition to optical propagation loss control by group index taper engineering. Future measurements will include determining the dynamic range of these sensors and applications in cancer diagnosis.

This work was supported by the National Cancer Institute Contract# HHSN261201200043C

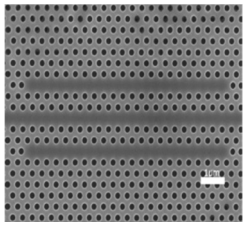

Fig. 1: SEM image of L21 coupled cavity

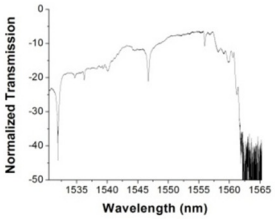

Fig. 2: Normalize transmission spectrum of L21 couple cavity

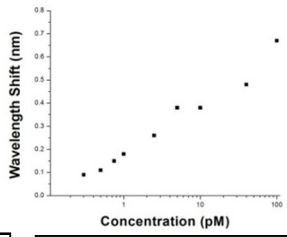

Fig. 3: Wavelength shift of resonance peak versus different concentrations

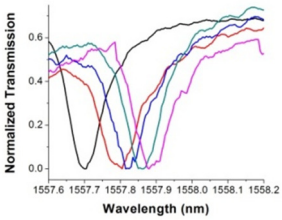

Fig. 4: Resonance wavelength shift at different concentrations

References:

[1] M. Iqbal et al "Label-Free Biosensor Arrays based on silicon ring resonators and high-speed optical scanning instrumentation", IEEE J. Sel. Top. Quant. Electron. 16(3), 654 (2010).

[2] A. Densmore et al "Silicon photonic wire biosensor array for multiplexed real-time and label-free molecular detection", Opt. Lett. 34(23), 3598 (2009).

[3] H. Sipova, et al, "Surface plasmon resonance biosensor for rapid label-free detection of microribonucleic acid at subfemtomole level", Anal. Chem. 82, 10110 (2010).

[4] S. Chakravarty, et al. "Slow Light Engineering for High Q High Sensitivity Photonic Crystal Microcavity Biosensors in Silicon." *Biosensors and Bioelectronics* 38,170 (2012)

[5] W-C. Lai, et al. "Silicon Nano-Membrane Based Photonic Crystal Microcavities for High Sensitivity Bio-Sensing." *Opt.Lett.* 37, 1208 (2012)

[6] C-Y. Lin, et al. "Wideband Group Velocity Independent Coupling into Slow Light Silicon Photonic Crystal Waveguide." *Applied Physics Letters* 97,183302 (2010)

[7] H. Subbaraman, et al. "Efficient Light Coupling into in-Plane Semiconductor Nanomembrane Photonic Devices Utilizing a Sub-Wavelength Grating Coupler." *Opt.Express* 20(18), 20659 (2012)

[8] Y. Zou et al, "High yield high sensitivity silicon-based photonic crystal microcavity bio-sensors", (In Review)